JACS
JOURNAL OF THE AMERICAN CHEMICAL SOCIETY

Article

pubs.acs.org/JACS

Groove Binding Mechanism of Ionic Liquids: A Key Factor in Long-Term Stability of DNA in Hydrated Ionic Liquids?

Aneesh Chandran, Debostuti Ghoshdastidar, and Sanjib Senapati*

Department of Biotechnology, Indian Institute of Technology Madras, Chennai 600036, India

Supporting Information

ABSTRACT: Nucleic acid sample storage is of paramount importance in biotechnology and forensic sciences. Very recently, hydrated ionic liquids (ILs) have been identified as ideal media for long-term DNA storage. Hence, understanding the binding characteristics and molecular mechanism of interactions of ILs with DNA is of both practical and fundamental interest. Here, we employ molecular dynamics simulations and spectroscopic experiments to unravel the key factors that stabilize DNA in hydrated ILs. Both simulation and experimental results show that DNA maintains the native B-conformation in ILs. Simulation results further suggest that, apart from the electrostatic association of IL cations with the DNA backbone, groove binding of IL cations through hydrophobic and polar interactions contributes significantly to DNA stability. Circular dichroism spectral measurements and fluorescent dye displacement assay confirm the intrusion of IL molecules into the DNA minor groove. Very interestingly, the IL ions were seen to disrupt the water cage around DNA, including the spine of hydration in the minor groove. This partial dehydration by ILs likely prevents the hydrolytic reactions that denature DNA and helps stabilize DNA for the long term. The detailed understanding of IL−DNA interactions provided here could guide the future development of novel ILs, specific for nucleic acid solutes.

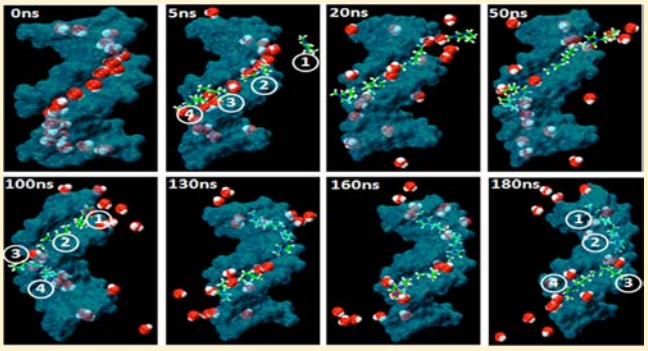

1. INTRODUCTION

DNA, apart from being a natural biological information carrier, has also been recognized as a key component in pharmaceutical and forensic realms and a crucial material in the development of advanced molecular devices.[1−3] For example, it has been reported that DNA vaccination confers protective immunity against infectious diseases, including AIDS and tuberculosis. Linear DNA has been shown to be useful as a structural linker for controlled aggregation of nanomaterials. The three-dimensional hydrogels made from flexible branched DNA building blocks have shown potential applications in tissue culture and drug delivery. Other potential uses include DNA-directed assembly of carbon nanotubues, DNA-programmed assembly of biomolecules, and DNA-based controllable nanostructures for the fabrication of artificial bionanomachines, devices, sensors, etc.

Despite these advantages, the long-term preservation of DNA under ambient conditions is a major challenge. Although DNA is considered to be reasonably stable in aqueous solution, it is susceptible to slow hydrolytic reactions, such as depurination and deaminaton, which can cause serious damage to the DNA structure.[4] Various other factors, such as temperature, pH, ionic strength, and solvent properties, can also disrupt the DNA helix and cause denaturation. Even in cryogenic storage, the DNA structure is found to be influenced by the storage temperature.[5] Dry storage of nucleic acids, which utilizes the basic natural principles of anhydrobiosis, is becoming a more attractive alternative to the conventional cold storage of DNA.[6] Nonetheless, there is a continuous inquest to develop suitable media for long-term preservation of DNA.

Ionic liquids (ILs) have found a wide range of applications in various fields, including organic synthesis, extraction/separation, electrochemical analysis, catalysis, protein purification, protein crystallization and detection, etc.[7] The applications of ILs to DNA technology have received tremendous attention in recent years. DNA separation using a capillary coated with imidazolium-based ILs and the use of ILs in designing ion-conductive DNA films have been reported.[8,9] ILs have also been reported to extract a trace amount of DNA from aqueous solutions and to slow DNA translocation through nanopores.[10,11] One of the most recent developments in the field is the use of ILs as ideal solvent media for long-term DNA storage. By spectroscopic measurements, MacFarlane and co-workers have demonstrated that the structural and chemical stability of DNA remain preserved up to one year in a series of choline-based ILs.[12] The effects of an IL on the DNA melting temperature (T_m) have also been investigated by these authors. Hence, an important bottleneck in the field is to understand the

Received: May 9, 2012
Published: November 26, 2012

   dx.doi.org/10.1021/ja304519d | J. Am. Chem. Soc. 2012, 134, 20330−20339

binding characteristics and molecular mechanism of interactions of IL molecules with DNA.

In this work, we combine molecular dynamics (MD) simulations, circular dichroism (CD) spectroscopy, UV−vis spectroscopy, and fluorescent dye displacement assay to unravel the key factors that stabilize DNA in hydrated ILs. Simulation results suggest that IL cations can enter the DNA grooves and contribute to DNA stability via hydrophobic and polar interactions. The CD spectral measurements and fluorescent dye displacement assay confirm the intrusion of IL molecules into the DNA minor groove. The mode of binding of IL cations to the minor groove resembles the binding of known DNA minor groove binders, such as netropsin, distamycin, 4′,6-diamidino-2-phenylindole (DAPI), etc. Interestingly, the IL ions were seen to disrupt the water cage around DNA, particularly the spine of hydration in the minor groove. This partial dehydration of DNA by IL ions likely prevents the hydrolytic reactions that denature DNA and helps stabilize DNA for a longer period. To the best of our knowledge, this is the first report of the intrusion of IL molecules into the DNA minor groove and its role in long-term DNA stability.

2. MATERIALS AND METHODS

2.1. Simulation Details. To start with, we performed a series of all-atom MD simulations of DNA in hydrated 1-butyl-3-methylimidazolium chloride, [BMIM][Cl]. [BMIM][Cl] is a good model IL on which a range of experiments have previously been performed.[13,14] Subsequently, four additional simulations were performed by varying the IL anions and cations to investigate different stabilization tendencies of IL ions on DNA. These ILs include [BMIM][NO_3], [BMIM][lactate], [choline][NO_3], and [choline][lactate]. Choline-based ILs were chosen due to recent experimental evidence of DNA stability in hydrated ILs by MacFarlane and co-workers.[12] The well-characterized Dickerson−Drew dodecamer (DD, 5′-d-(CGCGAATTCGCG)$_2$-3′) was chosen as a model DNA in simulations. DD is a very stable B-DNA duplex that contains a full helical turn and has been widely adopted as a general template.[15] The water:IL ratios in the simulations were again chosen on the basis of the concentrations of ILs in recent experiments.[12]

To build the initial structure of the control aqueous system, the DNA dodecamer was placed at the center of a cubic box of length 6.5 nm with periodic boundary conditions in all directions. A total of 22 sodium counterions and 8020 water molecules were added to fill the box. Sodium ions were placed 8 Å from the phosphorus atoms along the phosphate bisectors. The box size was chosen such that any DNA atom was at least 1.5 nm away from the box surface, preventing unwanted interactions with its image in translated unit cells. For the IL systems, the equilibrated dodecamer with four layers of surrounding water molecules from the aqueous system was placed into a cubic box of length 6.5 nm. This box was then filled with the requisite number of IL pairs and water to reach the desired IL concentrations. The systems were kept neutral by maintaining 22 Na^+ ions. Further details of the systems are presented in Table 1.

The Amber parm99 force field with parmbsc0 corrections[16] and TIP3P model were adopted to represent the interaction potentials of DNA and water, respectively. The interaction potentials used for BMIM- and choline-based ILs were adopted from the literature, in which they were developed within the spirit of the OPLS-AA/AMBER framework.[17,18] Simulations were carried out at 298 K and 1 atm of pressure. To enable the volume variation, simulations were performed in an NPT ensemble using the Berendsen thermostat and barostat. The calculation of long-range Coulombic forces was performed employing the full Ewald summation technique. The real space part of the Ewald sum and Lennard-Jones interactions were cut off at 15 Å. SHAKE was used to constrain bond lengths between heavy atoms and hydrogens. A set of minimization and thermalization runs of the starting structures were performed to remove the initial bad contacts.

Table 1. Details of the Simulated DNA-in-Hydrated IL Systems[a]

system	primary solvent component	[IL]:[water] (wt %)	no. of ILs	no. of water molecules
1	water	0:100		8020
2	[BMIM][Cl]	5:95	29	8020
3	[BMIM][Cl]	15:85	144	8020
4	[BMIM][Cl]	50:50	600	5816
5	[BMIM][Cl]	80:20	600	1454
6	[BMIM][NO_3]	80:20	600	1672
7	[BMIM][lactate]	80:20	600	1900
8	[choline][NO_3]	80:20	600	1380
9	[choline][lactate]	80:20	600	1605

[a]In systems 4−9, the IL concentrations are maintained similar to those in the experiments of MacFarlane and co-workers.[12]

Each system was thoroughly equilibrated until the potential energy and system volume ceased to show any systemic drift. Subsequently, a production phase of 200 ns was performed through the SANDER module of Amber 11.[19]

To compare the simulated DNA structures against the initial X-ray structure, we have calculated the root-mean-square deviation of the DNA molecule over the trajectories from the initial structure. Minor and major groove widths were calculated on the basis of the proposition of El Hassan and Calladine,[20] which involves the measurements of the cross-strand P−P′ distance (P_i−P'_{i-3} for the minor groove and P_i−P'_{i+4} for the major groove) with the necessary angle correction term. Sugar puckering was calculated by the method adopted by Altona and Sundaralingam,[21] where the phase angle of pseudorotation is computed from the five internal torsion angles of the sugar ring. Pairwise energy decompositions were performed for the nonbonded interactions to estimate the strength of regionwise DNA−IL interactions.

The free energy of binding of the IL pairs was computed from the simulation trajectories using the molecular mechanics Poisson−Boltzmann surface area (MMPBSA) approach.[22] For this purpose, a total of 5 windows with 100 snapshots at 10 ps intervals in each (i.e., last 5 ns of data) were taken from the trajectory and the interaction energies were calculated using the scripts available with the AMBER 11 program. The binding free energy (ΔG_{bind}) is obtained by taking the difference between the free energies of the DNA−IL complex ($G_{complex}$) and the unbound DNA ($G_{receptor}$) and IL pairs (G_{ligand}) and can also be calculated from the changes in the molecular mechanical gas-phase energy (ΔE_{MM}), entropic contribution, and solvation free energy:

$$\Delta G_{bind} = G_{complex} - G_{receptor} - G_{ligand} = \Delta E_{MM} - T\Delta S + \Delta G_{solv}$$

ΔG_{solv} is estimated by solving the linearized Poisson−Boltzmann equation for each of the three states (ΔG_{polar}) and adding an empirical term for hydrophobic contributions to it ($\Delta G_{nonpolar}$). The hydrophobic contribution is calculated from the solvent-accessible surface area. It is customary to neglect the entropic contribution, as the calculations involve binding of similarly charged molecules (ILs) to one particular DNA sequence.[23] Hence, the computed values will be termed the "relative binding free energy". For the calculation of ΔG_{polar}, the dielectric permittivities of the ILs were obtained from the literature.[24] It is worth mentioning here that, although path-based free energy methods, e.g., umbrella sampling and metadynamics, can provide more accurate measurements of ΔG_{bind}, they are computationally very expensive. However, in a system where the receptor and ligand do not undergo significant conformational changes upon binding (as in the present study), the MMPBSA approach has been proven to be a reliable and efficient method for determining relative binding free energies.[25]

2.2. Experimental Details. The experiments were performed with [BMIM][Cl] and calf thymus DNA (ct-DNA; ∼10 kbp). The reagents [BMIM][Cl], ct-DNA, and tris(hydroxymethyl)aminomethane (Tris)

dx.doi.org/10.1021/ja304519d | J. Am. Chem. Soc. 2012, 134, 20330−20339

were purchased from Sigma-Aldrich. The fluorescent dyes DAPI and Hoechst 33258 (H33258) were purchased from Polyscience (Niles, IL). The purchased sodium salt of ct-DNA was used without further purification, since the purity was sufficiently high as determined from optical measurements. The ratio of the absorbance of the DNA stock solution at 260 nm to that at 280 nm was found to be 1.88, indicating the absence of any protein. All other chemicals and solvents were of analytical grade.

All DNA samples were prepared in 5 mM Tris−HCl buffer (pH 7.4). A stock solution of DNA was prepared by dissolving ct-DNA in Tris−HCl buffer and stored at 4 °C for more than 24 h with gentle shaking to obtain homogeneity. DNA concentrations were determined by using an extinction coefficient of 6600 M^{-1} cm^{-1} at 260 nm and expressed in terms of base molarity.

2.3. CD and UV−Vis Spectroscopy. CD spectra were recorded on a J-810 Jasco spectropolarimeter at 25 °C using a rectangular quartz cell of 1 cm path length. Titrations were performed with a fixed concentration of ct-DNA (100 μM) and increasing concentrations of [BMIM][Cl]. Spectra shown were averaged over three successive scans recorded at a scan speed of 50 nm/min. Appropriate blanks were subtracted from the respective spectra, and the data were subjected to the noise reduction analysis. The absorption spectra of [BMIM][Cl] were recorded on a Perkin-Elmer Lambda-25 spectrophotometer at 25 °C. Here, a fixed concentration (50 μM) of [BMIM][Cl] was titrated with increasing concentrations of ct-DNA, and appropriate blanks were subtracted from the absorbance measurements.

2.4. Determination of Dye to Base Pair Stoichiometry. All fluorescence measurements were performed on a Molecular Devices Spectra Max Gemini spectrofluorometer with a 1 cm light path quartz cuvette. The probes, DAPI, and H33258 were titrated into the DNA solution (1 μg/mL) at increasing dye to base pair ratio (dbpr), and the fluorescence emissions were measured. As Figure S1 (Supporting Information) indicates, the fluorescence intensity initially increased with increasing dbpr until a ratio of 0.06 was reached and then leveled off.

2.5. Fluorescent Dye Displacement Assay. The dye displacement assay was performed using the methodologies adapted from the work of Boger et al.[26] The dye was mixed with ct-DNA (1 μg/mL) at the stoichiometric ratio. Different concentrations of [BMIM][Cl] were added, and each mixture was incubated for 30 min at 25 °C. The emission intensity was recorded for DAPI (excitation 358 nm, emission 468 nm, cutoff filter at 455 nm) and H33258 (excitation 348 nm, emission 480 nm, cutoff filter at 475 nm). Assessments were conducted in triplicate, and the fluorescence readings are reported as the percent fluorescent intensity decrease relative to the control (FI, %), i.e.

$$\mathrm{FI}\ (\%) = [(\mathrm{FI_T} - \mathrm{FI_C})/(\mathrm{FI_0} - \mathrm{FI_D})] \times 100$$

where FI_T, FI_C, FI_0, and FI_D are the fluorescent intensities of dye−DNA−IL, dye−IL, dye−DNA, and dye alone, respectively.

3. RESULTS AND DISCUSSION

3.1. Findings from MD Simulations. *3.1.1. Structure of DNA in ILs.* To check if DNA could maintain its native B-conformation in hydrated [BMIM][Cl], we have analyzed its structure along the simulation trajectories. As Figure S2 (Supporting Information) shows, the trajectories were stable (Figure S2a) and the sampled configurations were very close to the crystal structure (Figure S2b). The root-mean-square displacements (RMSDs) of the DNA from its initial position in the crystal structure were seen to converge during equilibration and merely oscillate around a mean value in the production phase of 200 ns (Figure S2a). Figure S2b shows a comparison of the time-averaged structures of DNA from IL solutions with the crystal structure. The averaged structures were obtained by taking the mean of the atom positions at every 25 ps interval during the last 50 ns run. The RMSD of the average structure of DNA in an 80 wt % IL solution was found to be only 1.53 Å. Even in the dilute solution of 5 wt % IL, the average RMSD of DNA was smaller than the RMSD value in an aqueous medium ($RMSD_{av}$ = 2.06 Å in IL vs 2.18 Å in water). More importantly, DNA was seen to maintain its canonical structure, keeping the groove dimensions and sugar puckering within the values expected for a B-DNA duplex (Figure S2c,d). The observed flexibility of the major and minor grooves is in good agreement with the general finding that groove plasticity is a key requirement to achieve good complementarity in its binding with ligands. As expected, the groove oscillations became more restricted in more concentrated IL solution due to the viscous nature of the medium[27](Figure S2c). The 2′-deoxyriboses mainly sampled the south and east regions, as expected for a B-DNA (Figure S2d).[15] Thus, the results suggest that the DNA retains its native B-conformation in hydrated [BMIM][Cl], which is in good agreement with the spectroscopic experiments of Ding et al.[13] and MacFarlane and co-workers.[12] The results also corroborate the simulation data of Cardoso and Micaelo, where the authors have noted the existence of the native DNA conformation in a variety of other ILs.[28]

3.1.2. Binding Characteristics of ILs to DNA. To understand the binding pattern of ILs to DNA, we considered various site−site radial distribution functions (RDFs). The RDFs of IL cations and anions have been calculated in three distinctly different regions of DNA: the phosphate backbone, major groove, and minor groove. Figure 1a shows the RDFs of IL ions in all three DNA regions. A significant population of IL ions in all three DNA regions, including the minor groove, is evident from the sharp first peaks in the RDFs. The graph also shows a preferential accumulation of IL cations over the anions in all regions. The large peaks for the phosphate−IL ions are not unexpected considering their ionic nature. However, the equally sharp peaks at almost the same distances for the groove−IL ions (barring the minor groove−IL anion), implying the intrusion of IL ions into the DNA grooves, deserve thorough investigations. The shifting of the minor groove−IL anion peak from 4.1 Å, the distance at which phosphate−anion and major groove−anion peaks occurred, is due to the unavailability of space filled by DNA backbone phosphates and their neighboring IL ion layers.

The spatial distribution maps of IL ions around DNA can provide direct evidence of the existence of IL ions in the DNA backbone and groove regions. Figure 1b presents a representative snapshot of the location of IL cations around DNA, picked up at 200 ns. As the figure implies, the IL cations established a major interaction with the phosphate groups of DNA. The calculated energy contributions imply that the nature of this interaction is primarily electrostatic (Table S1, Supporting Information), which corroborates other recent reports.[8,10,29,30] It is evident from Figure 1 that $[BMIM]^+$ cations also associate with the major groove of DNA. A combination of electrostatic and van der Waals interactions was seen to operate at this site of DNA (see Table S1). A significant number of H-bonds were also found to exist between the DNA major groove and IL cations, which mainly involved the oxygen and nitrogen of guanine and oxygen of thymine as the acceptors and the carbon atoms in the imidazolium ring as donors (Table S2, Supporting Information). A comparatively weaker association of thymine may presumably be due to the presence of the bulky methyl group.

dx.doi.org/10.1021/ja304519d | J. Am. Chem. Soc. 2012, 134, 20330−20339

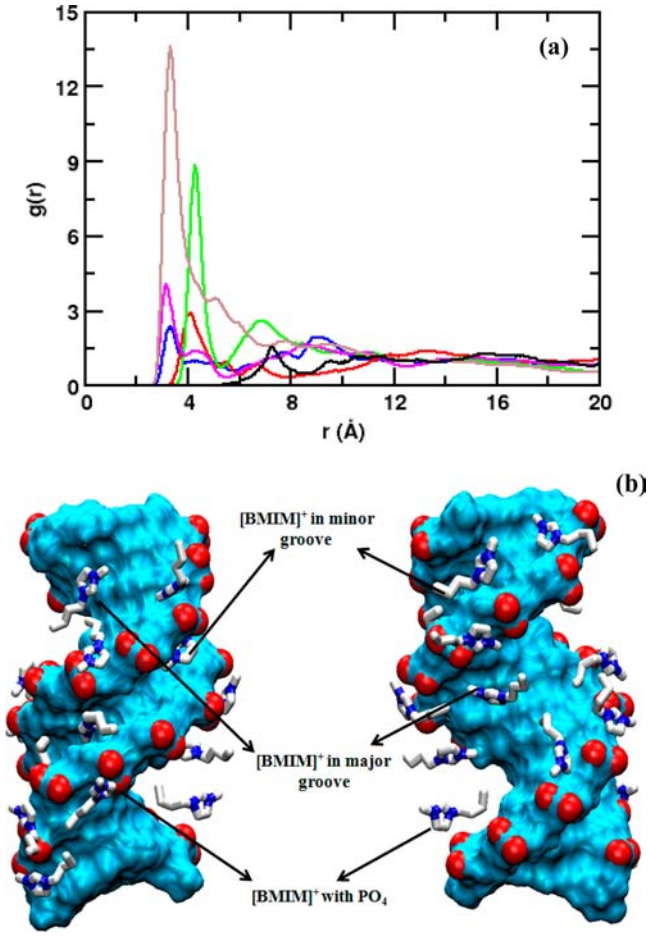

Figure 1. (a) Radial distribution functions (RDFs) of IL ions in different DNA regions. Color scheme: cation−phosphate, brown; cation−major groove, magenta; cation−minor groove, blue; anion−phosphate, green; anion−major groove, red; anion−minor groove, black. The following sites were considered for calculating the RDFs: center-of-mass (COM) of the imidazolium ring for the cation, Cl^- for the anion, P for the phosphate group, electronegative sites N3 and O2 for the minor groove, and electronegative sites N7, O6, and O4 for the major groove. The distribution is shown for the 80 wt % [BMIM][Cl] solution. (b) Representative spatial distribution map of IL cations showing their association with the DNA backbone, major groove, and minor groove. A similar distribution has been noted throughout the simulation trajectory, as included in Figure S3 (Supporting Information). Color scheme: cyan, DNA; red, DNA phosphates; white, IL cations; blue, ring nitrogens of the IL cations.

Interestingly, a few $[BMIM]^+$ cations were found to occupy the DNA minor groove as well (Figure 1). These cations entered the minor groove over the course of the simulation and remained bound to the groove without disturbing the double helical structure of DNA. Even in the most dilute solution of 5 wt % IL, at least two cations were found to occlude the minor groove of the dodecamer. In concentrated 80 wt % solution, four such cations were found at any given time. Figure S4 (Supporting Information) shows the time evolution of these minor-groove-occupying IL cations. Although these cations could exchange among themselves in dilute solutions, they appear to be stable within the minor groove of DNA in concentrated solutions.

Figure S5 (Supporting Information) provides a closer view of the alignment of these cations in the minor groove. The imidazolium ring lied perpendicular to the groove with the cationic carbon atoms (either C2 or C3 and C4) pointing toward the bases. In this orientation, the C−H of the imidazolium ring forms hydrogen bonds with the acceptor groups in the nucleotides. However, the geometries of these hydrogen bonds were found to depart significantly from linearity since, in most cases, these interactions involved three sites. For example, a three-centered bifurcated H-bond was seen to be prevalent between C−H and the pair of adenine N3 and thymine O2 or between C−H and the pair of adenine N3 and cytosine O2. Some of these three-centered hydrogen bonds formed a bridge between the bases and ribose sugars of the two opposite DNA strands through the electronegative sites in bases and O4′ atom in riboses. Three-centered hydrogen bonds were also observed for the bases and riboses of the same strand (Figure S4c, Supporting Information). Such an intrusion of $[BMIM]^+$ cations into the DNA minor groove and their mode of interactions resemble the binding of known DNA minor groove binders DAPI, netropsin, distamycin, etc.[31,32] Table S2 (Supporting Information) lists the occurrences (%) of these hydrogen bonds. As the table indicates, the IL cations spend more time with adenine and cytosine with average occurrences of H-bonds of >60%. Such a preferential H-bonding was also noted for many known minor groove binders.[31] The presence of the bulky $-NH_2$ group makes guanine the least accessible H-bond partner. Owing to the perpendicular orientation of $[BMIM]^+$ cations with respect to the groove bases, cationic carbon atoms on the opposite face of the imidazolium ring (i.e., C3 and C4 when C2 is hydrogen bonded to bases and vice versa) are exposed to the bulk and form H-bonds with water. The proximity and parallel facing of the alkane groups of $[BMIM]^+$ cations to the ribose sugar rings imply the possible existence of weak CH$\cdots\pi$ interactions as well.

Overall, the results from Figures 1 and S3 and S4 (Supporting Information) indicate that, irrespective of the concentration of our model IL in solution, a certain fraction of IL cations always enter the DNA minor groove. The finding was further strengthened by simulating two different sequences of the DNA dodecamer (5′-d(GCAAACGTTTGC)$_2$-3′ and 5′-d(CTCGGCGCCATC)$_2$-3′) in 80 wt % [BMIM][Cl] solution, where a similar IL intrusion into DNA minor groove was observed (Figure S6, Supporting Information). The computed interaction energies (Table S1, Supporting Information) show that the electrostatic interactions between the IL and DNA backbone, alongside a combination of hydrophobic and polar interactions between the IL and DNA major and minor grooves, contribute to DNA stability.

3.1.3. DNA Solvation by ILs. Hydration plays a crucial role in the three-dimensional structural stability of DNA and also in the assembly of different polymorphic forms of the double helix and their conformational dynamics. To understand the nature of DNA hydration in IL solutions, we have investigated the distribution of water and IL cations around DNA. Parts a and b of Figure 2 show representative spatial distribution maps of water and IL cations in the first solvation layer of DNA, defined as a shell of 3.5 Å. The figure clearly demonstrates that IL cations penetrate the hydration layer and take part in the DNA solvation mechanism. In 5 and 80 wt % IL solutions, on average about 5 and 47 $[BMIM]^+$ cations entered the first solvation layer, respectively, and colocalized with water and Na^+ ions. The so-called "cone of hydration", the tetrahedral arrangement of water molecules around the charged phosphate groups,[33] was greatly disturbed with the entry of IL cations. As the concentration increases, the IL population rises significantly

dx.doi.org/10.1021/ja304519d | J. Am. Chem. Soc. 2012, 134, 20330−20339

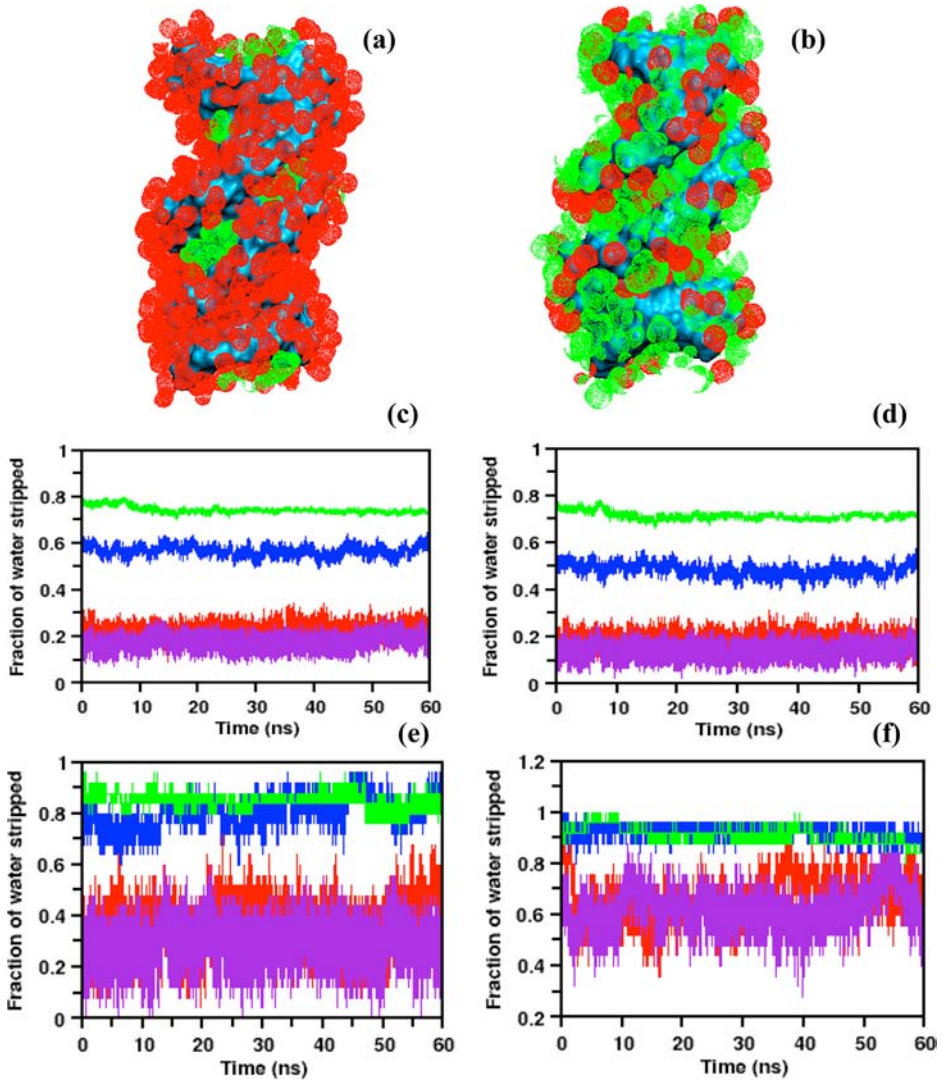

Figure 2. Spatial distribution of water and IL cations around DNA in (a) 5 wt % and (b) 80 wt % IL solutions. The representative distribution at 200 ns is very similar to the other randomly picked distributions at different simulation times. Color scheme: cyan, DNA; red, water; green, imidazolium moiety of IL cations. (c–f) Fraction of water stripped from various regions of DNA at different IL concentrations: (c) from DNA, (d) from the DNA sugar–phosphate backbone alone, (e) from the DNA major groove alone, and (f) from the DNA minor groove alone. Color scheme: violet, 5 wt % IL solution; red, 15 wt % IL solution; blue, 50 wt % IL solution; green, 80 wt % IL solution. The fraction of water stripped was calculated from the fraction of water present, which in turn was calculated by counting the water present within 3.5 Å of a specific region and normalizing that value with the water count in the control DNA-in-water system. Results are shown for the final 60 ns for clarity.

in the solvation layer, stripping off a considerable amount of water from the DNA surface (Figure 2a,b). A plausible explanation is that more electropositive IL cations experience stronger attraction toward the negatively charged DNA duplex backbone as well as toward the DNA major and minor grooves, which are rich in H-bonding functional groups (Tables S1 and S2, Supporting Information). Such a strong affinity helps the IL cations to disrupt the well-coordinated hydration layer around DNA and take part in the solvation process.

To obtain further details about the extent of water displacement by [BMIM][Cl], we have calculated the number of water molecules stripped from the DNA solvation shell as a function of the simulation time. Results are shown for all the systems, including the control system of DNA in pure water. As shown in Figure 2c, more than 75% water molecules were stripped off by IL cations in the solution of 80 wt % [BMIM][Cl]. Regionwise population analysis provides a clearer view of water decrement in and around DNA. Parts d–f of Figure 2 show the fraction of water stripped from the DNA sugar–phosphate backbone, major groove, and minor groove, respectively. The reduction in water content at the three respective regions was computed to be ~70%, 83%, and 88% for the 80 wt % solution. It is noteworthy that, even at higher concentrations of ILs, about 25% water is retained in the first hydration layer of DNA. The presence of such a small amount of water in the IL media was reported to be necessary for maintaining the structural and functional integrity of biomolecules.[12,34,35]

3.1.4. Spine of IL Cations. Prior structural studies have revealed the presence of a well-ordered hydration network, called the "spine of hydration", in the DNA minor groove.[36,37] The spine of hydration was first reported by Drew and Dickerson in the crystal structure of B-DNA, which consisted of two layers of ordered water aligned along the minor groove.[36] Our control simulation of DNA in pure water could successfully reproduce the spine of water, as shown in Figure

dx.doi.org/10.1021/ja304519d | J. Am. Chem. Soc. 2012, 134, 20330–20339

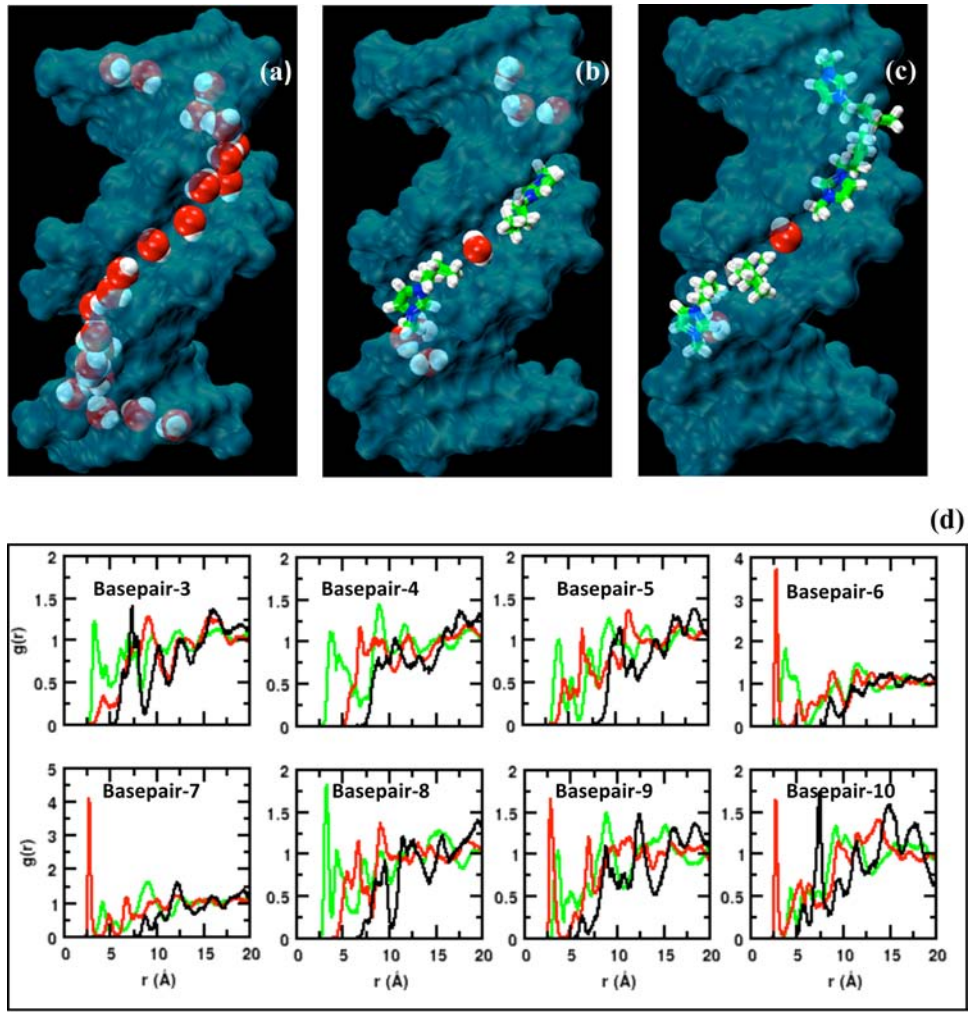

Figure 3. (a) Spine of hydration in the minor groove of DNA from control simulation. Emergence of the "water-assisted spine of $[BMIM]^+$ cations" in the DNA minor groove is shown for (b) 5 wt % and (c) 80 wt % IL solutions. A more detailed description of the formation of such a spine of IL is shown in Figure S7 and Movie S1 (Supporting Information). (d) Radial distribution functions of DNA base pairs−IL ions/water in the minor groove of the 80 wt % solution. Color scheme: green, IL cations; black, IL anions; red, water. The following sites were considered: $COM_{imidazolium}$, Cl^-, O_{water}, guanine N3 and cytosine O2 for base pairs 3, 4, 9, and 10, and adenine N3 and thymine O2 for base pairs 5−8.

3a. The primary water layer was hydrogen-bonded to the adenine N3 nitrogen and/or thymine O2 oxygen and then reached across the minor groove to a second N3 nitrogen or O2 oxygen in the opposite strand, one base pair displaced. The second water layer bridged the water oxygens of the primary hydration layer to the bulk water. As the figure indicates, the spine is not only restricted to the central AT sequence but also extends to the flanking CGCG sequence, which is consistent with the common findings.[38]

Interestingly, the $[BMIM]^+$ cations in IL solutions were seen to disrupt the spine of hydration by intruding into the DNA minor groove. The spine of water was displaced by a water-assisted spine of IL cations, irrespective of the concentration of IL in solution. Parts b and c of Figure 3 show the representative structures of DNA bound to the spine of $[BMIM]^+$ ions in 5 and 80 wt % solutions. The structures were picked up at the end of the simulations at 200 ns. Figure S7 (Supporting Information) shows the time evolution of the formation of such a spine of IL in 80 wt % solution. During equilibration and the initial 50 ns of the production phase, the IL cations compete with waters of the native spine of hydration in the minor groove. However, once the water molecules are displaced, the IL cations are seen to settle down in the minor groove and remain so thereafter till the end of the simulations (also see Movie S1, Supporting Information). Computed RDFs, shown in Figure 3d, also support the existence of a water-assisted spine of IL cations. Site−site RDFs, comprising the center-of-mass (COM) of the imidazolium ring of IL cations and the electronegative sites (N3 and O2) in the bases, show that the IL cations are in close contact with base pairs 3, 4, 5, 8, and 9 in the minor groove of the DNA dodecamer. The RDFs for the base pairs 6 and 7, on the other hand, show the dominance of water−minor groove interactions at these sites. Overall, a significant amount of water is displaced from the minor groove, and a spine of IL cations takes over. A similar phenomenon of water displacement from the spine of hydration was reported for the drugs that target the DNA minor groove.[39] A combination of electrostatic and hydrophobic interactions, as discussed above under the subsection "Binding Characteristics of ILs to DNA", drives the $[BMIM]^+$ ions to the DNA minor groove. A more quantitative description of water stripping from the minor groove can be seen from Figure 2f. A comparison of part f with parts d and e of Figure 2 shows that, while a significant amount of water is stripped from the DNA backbone

dx.doi.org/10.1021/ja304519d | J. Am. Chem. Soc. 2012, 134, 20330−20339

and major groove only at higher IL concentrations, more than 50% of the water is displaced from the minor groove even at an IL concentration of 5 wt %. At higher [BMIM][Cl] concentrations, about 90% of the water molecules are displaced from the minor groove, leaving a well-ordered spine of IL molecules. Such a partial dehydration of DNA by ILs, particularly from the minor groove, could prevent hydrolytic reactions such as depurination and deamination and impart conformational stability to DNA.

3.1.5. Effect of the IL Ion Type on DNA Stability. DNA was simulated in two additional [BMIM]-based ILs, [BMIM][NO_3] and [BMIM][lactate], to investigate the effects of an IL anion on DNA stability (Table 1). Both these systems were simulated for 100 ns after extensive equilibration by following the same protocol as described for the DNA-in-[BMIM][Cl] system. The DNA conformation and the mode of binding of ILs to DNA were examined by performing analyses similar to those described above. DNA was seen to retain its native B-conformation in both the systems, and ILs participated in strong interactions with the DNA backbone and grooves. Moreover, irrespective of the anion type, $[BMIM]^+$ ions always intruded into the DNA minor groove (Figure S8, Supporting Information). The conformational stability imparted by IL molecules to DNA can be quantified through the strength of their interactions, which can be estimated from the free energy of binding of ILs to DNA. For this purpose, we computed the binding Gibbs energy of ILs present within the first solvation shell of DNA by the molecular mechanics Poisson–Boltzmann surface area approach. The relative binding energy values (ΔG_b) tabulated in Table 2 show that [BMIM][Cl] and [BMIM][NO_3] bind to DNA more strongly than [BMIM]-[lactate], implying the presence of an anion effect on DNA stability in ILs.

Table 2. Free Energy of Binding of IL Pairs to the DNA Dodecamer in Different DNA-in-IL Systems (Systems 5–9)

system	ΔG_b (kcal/mol)
[BMIM][Cl]	−8.96 ± 0.72
[BMIM][NO_3]	−8.53 ± 0.81
[BMIM][lactate]	−7.18 ± 0.74
[choline][NO_3]	−7.83 ± 0.60
[choline][lactate]	−6.17 ± 0.68

To investigate the effects of anions further, we simulated DNA in two choline-based ILs, [choline][NO_3] and [choline]-[lactate], under the same experimental conditions as those used by MacFarlane and co-workers. A similar protocol for simulation and analyses was executed as described above. Again, DNA was seen to retain its native B-conformation in both the systems, and [choline] cations were found to intrude into the DNA minor groove. The nature of binding of these cations to the DNA minor groove is shown in Figure S8 (Supporting Information). It is clear from Figure S8c,d that [choline] cations do not fit into the DNA minor groove as nicely as the [BMIM] cations, due to the presence of a bulky tetrahedral $N(Me)_3$ headgroup. Conversely, $[BMIM]^+$ can bind to the minor groove more effectively because of its (almost) planar geometry and better charge delocalization on the imidazolium ring, by which it can make a larger number of contacts with the base of the groove. This implies a greater stabilization tendency of [BMIM] cations on DNA relative to the [choline] cations. Such a differential tendency is also reflected in the free energy of binding values in Table 2, where for a given anion [BMIM] cations show stronger binding with DNA. The influence of anions on DNA stability was also evident from binding energy values of the [choline]-based ILs, where [choline][NO_3] shows stronger interaction with DNA than [choline][lactate]. It was encouraging to see that our computed free energy values are in good agreement with recently determined ΔG_b values of [BMIM][Br] to DNA by fluorescence measurements.[29]

As a consequence of IL penetration into the DNA hydration layer, in all these systems, a large number of water molecules were stripped off, similar to the primary DNA-in-[BMIM][Cl] system. Figure 4 shows the extent of water displacement by

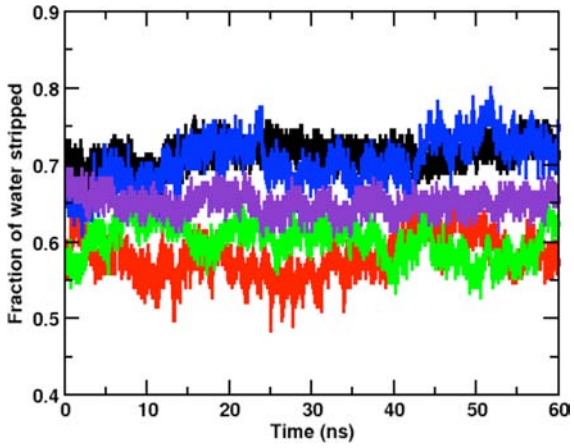

Figure 4. Fraction of water stripped from the solvation shell of the DNA dodecamer dissolved in different 80 wt % IL systems. Color scheme: black, [BMIM][Cl]; red, [BMIM][NO_3]; green, [BMIM]-[lactate]; blue, [choline][NO_3]; indigo, [choline][lactate]. The fraction of water is calculated similarly to that in Figure 2. Results from the last 60 ns are shown for clarity.

these ILs as a function of the simulation time. About 55–75% of the water molecules were stripped from the solvation shell of DNA. It should be noted that the extent of water displacement does not necessarily depend only on the strength of the interactions. It also depends on the amount of IL ions penetrating the DNA solvation layer. To support this, we have calculated the number of IL cations and anions present in the DNA solvation shell, and they are presented in Figure S9 (Supporting Information). It is worth noting that the extent of water stripping is nearly proportional to the number of IL cations present in the DNA solvation shell, except in the [choline][lactate] system. However, a closer look at the IL anion distribution (Figure S9b) shows that the population of anions in the [choline][lactate] system is largest among all the systems studied and the number of cations and anions is almost the same. This can imply that the ion-pairing effect is very strong in [choline][lactate]. To validate this, we have simulated the same five neat ILs without DNA. The cation–anion radial distribution functions, as presented in Figure S10 (Supporting Information), shows the largest first peak for [choline][lactate] occurring at <3.5 Å, suggestive of the existence of strong H-bonding due to the −OH group in both the ions. Now, recall that the number of IL cations present in the DNA solvation shell is larger than the number of anions in all systems (Figure S9). Thus, combining the ΔG_b values from Table 2 and the ion distribution in Figure S9, one can infer that both IL cations and

dx.doi.org/10.1021/ja304519d | J. Am. Chem. Soc. 2012, 134, 20330–20339

anions influence the DNA stability in ILs, but cations play the lead role.

3.2. Experimental Verification of DNA Structure and IL Minor Groove Binding. We performed spectroscopic experiments to verify our findings from MD simulations, particularly the structure of DNA in IL solutions and the minor groove binding of ILs. ct-DNA was used for all the experiments, and [BMIM][Cl] was taken as the model IL. The results are presented below.

3.2.1. Structure of DNA in ILs: CD Spectroscopic Analysis. Circular dichroism spectra of ct-DNA in hydrated [BMIM][Cl] of different concentrations ranging from 5 to 80 wt % and in an aqueous solution control were recorded. As Figure 5 indicates,

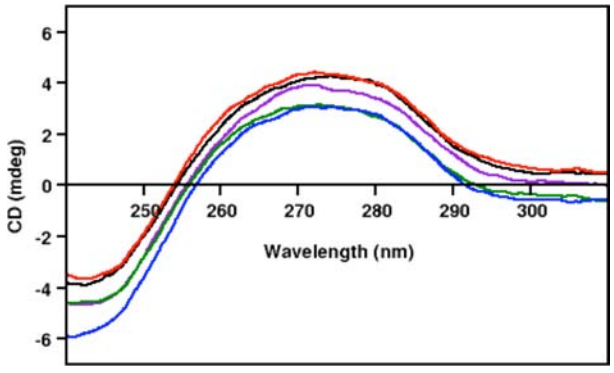

Figure 5. CD spectra of ct-DNA (100 μM) in water and hydrated [BMIM][Cl] solutions. Color scheme: black, water; red, 5 wt % IL solution; purple, 15 wt % IL solution; green, 50 wt % IL solution; blue, 80 wt % IL solution.

the characteristic positive band at ~275 nm corresponding to base stacking and a short-wave, negative band at ~245 nm (with a crossover at 258 nm) corresponding to helicity were present in all cases. This indicates that DNA retains its B-conformation in hydrated [BMIM][Cl] solutions. Our finding corroborates the experimental results of Ding et al.[13] and MacFarlane and co-workers[12] and more importantly validates our simulation results that the native B-conformation of DNA remains intact in hydrated ILs. The slight decrease in the dichroic signal at higher IL concentrations may be attributed to strong interactions of IL cations with DNA, which could lead to a transition from the extended double helix to the more compact form known as the Ψ structure.[13,40] The absence of any noticeable induced signal in the DNA region of the CD spectra indicates that IL cations do not intercalate.[41]

3.2.2. Binding Characteristics of ILs to DNA: Absorption Spectra. In recent years, studies have been carried out to understand the optical properties of the imidazolium cation based ILs. The absorption characteristics of these liquids are attributed to the imidazolium moiety of the cations.[14] In general, binding of small molecules to DNA produces hypochromic and bathochromic shifts in the absorption band of the bound ligand. The bathochromic shift is particularly dominant for intercalators.[42] We recorded the absorption spectra of [BMIM][Cl] in the absence and presence of ct-DNA in 5 mM Tris–HCl buffer, and the results are presented in Figure 6. The aqueous solution of ILs shows a broad spectrum in the range of 202–230 nm with a maximum at 211 nm. With addition of ct-DNA to the solution, the absorbance decreases with the maximum shifting from 211 to 214 nm. Such a decrease in the absorption, followed by a red shift in the

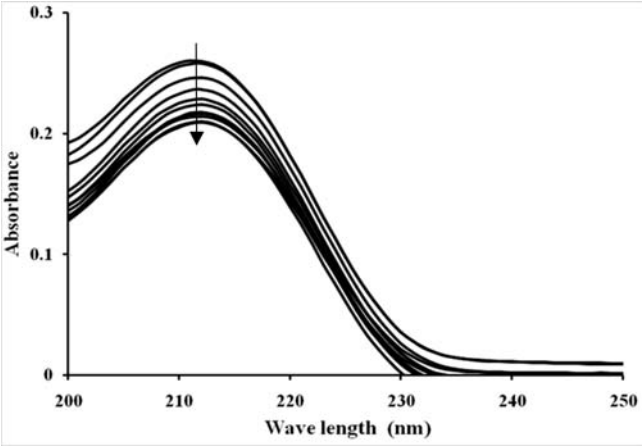

Figure 6. Change in UV–vis absorption spectra of [BMIM][Cl] (50 μM) in the absence (top curve) and presence of ct-DNA (5, 10, 15, 20, 30, 40, 50, 60, 70, and 80 μM) in 5 mM Tris–HCl buffer. The arrow shows the absorbance change with increasing DNA concentration.

absorption maximum, indicates the relocation of IL molecules to a nonpolar environment upon addition of ct-DNA. As the CD spectral data ruled out the possibility of intercalation, the probable mode of binding of ILs to DNA is through the minor groove. Moreover, in general, a large bathochromic shift implies the intercalation of ligand into the base stack of DNA, and the small shift of 3 nm in this case could be due to the groove binding rather than the intercalation of IL cations.

3.2.3. Minor Groove Binding of ILs to DNA: Fluorescent Dye Displacement Assay. Thus far, (i) MD simulation data showed that the IL cations can enter into the DNA minor groove and (ii) the absence of any noticeable induced signal in the DNA region of CD spectra implies that IL cations do not intercalate.[41] Combining (i) and (ii), one can infer that minor groove binding of ILs is very likely, which we attempt to confirm by fluorescent dye displacement assay.

Fluorescent dye displacement assay has attracted much attention as a simple, nondestructive, and high-throughput technique to establish the binding properties of small molecules to DNA.[22] The technique entails the measurement of the loss of fluorescence derived from the displacement of intercalators or minor groove binders by the DNA binding compounds. The compound displaces the probe if it competes for the same binding site in DNA. Here, we performed the assay to confirm the minor groove binding of ILs to DNA. For this purpose, we have chosen two minor groove binding probes, DAPI and H33258. The results are shown in Figure 7 in terms of the relative decrease in fluorescence (%) of DNA-bound DAPI and H33258 when different concentrations of [BMIM][Cl] were added to the solution. As Figure 7 shows, the fluorescence intensities of both DAPI and H33258 decrease with increasing IL concentration, indicating that the IL molecules enter the minor groove and displace DAPI and H33258 (though at molar concentrations). This confirms the participation of ILs in DNA stability through the minor groove binding. Such a close association of charged IL moieties with the DNA backbone and minor groove likely screens the interstrand repulsions between charged phosphate groups and helps stabilize B-DNA.

dx.doi.org/10.1021/ja304519d | J. Am. Chem. Soc. 2012, 134, 20330–20339

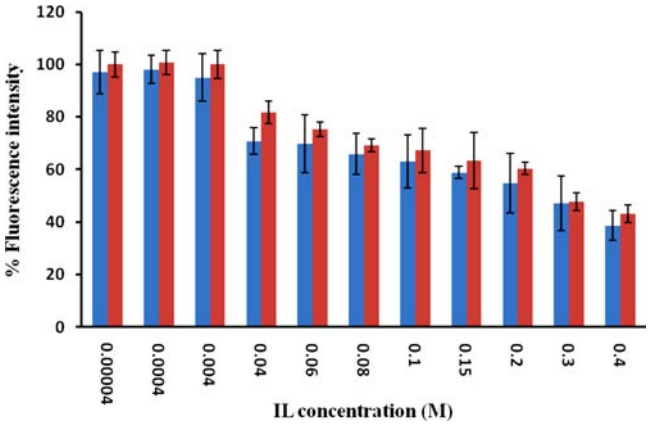

Figure 7. Relative decrease in fluorescence of DNA-bound dyes, titrated with increasing concentration of [BMIM][Cl]. The dye to base pair ratio used was 0.06 for DAPI and H33258. Color scheme: blue, DAPI; maroon, H33258. Error bars are shown.

4. SUMMARY AND CONCLUSIONS

The basis of long-term stability of DNA in hydrated ILs is explored via MD simulations and spectroscopic experiments. The results suggest that the groove binding mechanism of IL cations contributes significantly to DNA stability, in addition to their electrostatic association with the DNA backbone. The interaction of ILs with the minor groove is via hydrogen bonding, van der Waals contacts, and electrostatic effects of the IL cation, carrying a +1 charge. The high density of IL cations in the DNA solvation shell screens the interstrand phosphate repulsions and helps stabilize the B-conformation of DNA. Moreover, the partial dehydration of DNA by ILs likely prevents the hydrolytic reactions that denature DNA. The strong IL cation−DNA interactions not only lock the DNA in the B-conformation but also prevent intermolecular interactions between the neighboring DNA strands, a phenomenon known to be inevitable for the B to A conformational transition. Hence, despite severe dehydration, the B-DNA conformation is maintained in hydrated ILs.[13,43] Our finding of DNA dehydration is supported by the recent report that the mechanism of DNA dry storage follows the principle of anhydrobiosis[6]—"life without water". Nevertheless, a more direct verification of water stripping from the DNA solvation shell will be a focus of our future research.

■ ASSOCIATED CONTENT

Ⓢ Supporting Information

Tables S1 and S2 giving the IL cation−DNA interaction energies and percent occupancies of hydrogen bonds between $[BMIM]^+$ cations and DNA bases, Figures S1−S10 showing the relative fluorescent intensities of DAPI and H33258, structural characterizations of DNA, distribution of $[BMIM]^+$ cations around DNA, intrusion of IL cations into the DNA minor groove, schematic representation of $[BMIM]^+$−5′-d-$(CGCGAATTCGCG)_2$-3′ interactions, intrusion of $[BMIM]^+$ cations into the DNA minor groove irrespective of the base sequence, time evolution of the formation of a "water-assisted spine of IL cations" in place of a "spine of hydration" in the DNA minor groove, representative snapshots of IL cation binding to the minor groove of DNA, number of IL cations and IL anions in the solvation shell of DNA for different IL systems, and cation−anion RDFs in neat ILs, Movie S1 showing the stripping of water by IL cations from the DNA minor groove and the formation of a water-assisted spine of IL cations in the DNA minor groove (MPG), and complete ref 19. This material is available free of charge via the Internet at http://pubs.acs.org.

■ AUTHOR INFORMATION

Corresponding Author

sanjibs@iitm.ac.in

Notes

The authors declare no competing financial interest.

■ ACKNOWLEDGMENTS

The financial support of the Department of Science and Technology (DST), Government of India, is gratefully acknowledged. A.C. is thankful to the University Grants Commission, Government of India, for a research fellowship. We sincerely thank Mr. Hemant Giri, Ms. Archana Sundararaghavan, Dr. Nitish R Mahapatra, Dr. Madhulikha Dikshit, and Dr. G. K. Suraishkumar for their help with the experiments.

■ REFERENCES

(1) Kutzler, M. A.; Weiner, D. B. *Nat. Rev. Genet.* **2008**, *9*, 776−788.
(2) Jobling, M. A.; Gill, P. *Nat. Rev. Genet.* **2004**, *5*, 739−751.
(3) Krishnan, Y.; Simmel, F. C. *Angew. Chem., Int. Ed.* **2011**, *50*, 3124−3156.
(4) Lukin, M.; de los Santos, C. *Chem. Rev.* **2006**, *106*, 607−686.
(5) Roder, B.; Fruhwirth, K.; Vogl, C.; Wagner, M.; Rossmanith, P. *J. Clin. Microbiol.* **2010**, *48*, 4260−4262.
(6) Bonnet, J.; Colotte, M.; Coudy, D.; Couallier, V.; Portier, J.; Morin, B.; Tuffet, S. *Nucleic Acids Res.* **2010**, *38*, 1531−1546.
(7) Kokorin, A., Ed. *Ionic Liquids: Applications and Perspectives*; InTech: Rijeka, Croatia, 2011.
(8) Qin, W.; Li, S. F. Y. *Analyst* **2003**, *128*, 37−41.
(9) Nishimura, N.; Nomura, Y.; Nakamura, N.; Ohno, H. *Biomaterials* **2005**, *26*, 5558−5563.
(10) Wang, J. H.; Cheng, D. H.; Chen, X. W.; Du, Z.; Fang, Z. L. *Anal. Chem.* **2007**, *79*, 620−625.
(11) de Zoysa, R. S. S.; Jayawardhana, D. A.; Zhao, Q.; Wang, D.; Armstrong, D. W.; Guan, X. *J. Phys. Chem. B* **2009**, *113*, 13332−13336.
(12) Vijayaraghavan, R.; Izgorodin, A.; Ganesh, V.; Surianarayanan, M.; MacFarlane, D. R. *Angew. Chem., Int. Ed.* **2010**, *49*, 1631−1633.
(13) Ding, Y.; Zhang, L.; Xie, J.; Guo, R. *J. Phys. Chem. B* **2010**, *114*, 2033−2043.
(14) Paul, A.; Mandal, P. K.; Samanta, A. *J. Phys. Chem. B* **2005**, *109*, 9148−9153.
(15) Perez, A.; Luque, F. J.; Orozco, M. *J. Am. Chem. Soc.* **2007**, *129*, 14739−14745.
(16) Perez, A.; Marchan, I.; Svozil, D.; Sponer, J.; Cheatham, T. E., III; Laughton, C. A.; Orozco, M. *Biophys. J.* **2007**, *92*, 3817−3829.
(17) Lopes, J. N. C.; Padua, A. A. H. *J. Phys. Chem. B* **2006**, *110*, 19586−19592.
(18) Sambasivarao, S. V.; Acevedo, O. *J. Chem. Theory Comput.* **2009**, *5*, 1038−1050.
(19) Case, D. A.; et al. *AMBER 11*; University of California: San Francisco, 2010.
(20) El Hassan, M. A.; Calladine, C. R. *J. Mol. Biol.* **1998**, *282*, 331−343.
(21) Altona, C.; Sundaralingam, M. *J. Am. Chem. Soc.* **1972**, *94* (23), 8205−8212.
(22) Kollman, P. A.; Massova, I.; Reyes, C.; Kuhn, B.; Huo, S.; Chong, L.; Lee, M.; Lee, T.; Duan, Y.; Wang, W.; Donini, O.; Cieplak, P.; Srinivasan, J.; Case, D. A.; Cheatham, T. E., III. *Acc. Chem. Res.* **2000**, *33*, 889−897.
(23) (a) Wang, J.; Morin, P.; Wang, W.; Kollman, P. A. *J. Am. Chem. Soc.* **2000**, *123*, 5221−5230. (b) Mascarenhas, N. M.; Kastner, J. *BMC Struct. Biol.* **2012**, *12*, 8.
(24) (a) Huang, M.-M.; Jiang, J.; Sasisanker, P.; Driver, G. W.; Weingartner, H. *J. Chem. Eng. Data* **2011**, *56*, 1494−1499. (b)

Dielectric constants used for MMPBSA calculations are as follows: [BMIM][Cl], 15; [BMIM][NO_3], 15; [BMIM][lactate], 40; [choline][NO_3], 44; [choline][lactate], 69.
(25) Treesuwan, W.; Wittayanarakul, K.; Anthony, N. G.; Huchet, G.; Alniss, H.; Hannongbua, S.; Khalaf, A. I.; Suckling, C. J.; Parkinson, J. A.; Mackay, S. P. *Phys. Chem. Chem. Phys.* **2009**, *11*, 10682−10693.
(26) Boger, D. L.; Fink, B. E.; Brunette, S. R.; Tse, W. C.; Hedrick, M. P. *J. Am. Chem. Soc.* **2001**, *123*, 5878−589.
(27) To check that, at higher IL concentrations, particularly at 80 wt % solution, the DNA is not constrained within a glassy matrix of IL, we have calculated the self-diffusion coefficients of IL ions from their mean squared displacements (MSDs). The obtained diffusivity values of $(0.21 \pm 0.04) \times 10^{-11}$ and $(0.14 \pm 0.02) \times 10^{-11}$ m^2/s for $[BMIM]^+$ and $[Cl]^-$, respectively, match favorably with the experimental self-diffusivity value of 0.68×10^{-11} m^2/s for $[BMIM]^+$ in [BMIM][PF_6] (Tokuda, H.; Hayamizu, K.; Ishii, K.; Susan, M. A. B. H.; Watanabe, M. *J. Phys. Chem. B.* **2004**, *108*, 16593−16600), suggesting that the desired diffusive regime has been reached. Presumably, the presence of water helped attain the equilibrium phase relatively quickly, compared to neat IL systems. The self-diffusivity of water, in this system, was calculated to be $(1.70 \pm 0.02) \times 10^{-11}$ m^2/s.
(28) Cardoso, L.; Micaelo, N. M. *ChemPhysChem* **2011**, *12*, 275−277.
(29) Wang, H.; Wang, J.; Zhang, S. *Phys. Chem. Chem. Phys.* **2011**, *13*, 3906−3910.
(30) Xie, Y. N.; Wang, S. F.; Zhang, Z. L.; Pang, D. W. *J. Phys. Chem. B* **2008**, *112*, 9864−9868.
(31) Neidle, S. *Nat. Prod. Rep.* **2001**, *18*, 291−309.
(32) Dolenc, J.; Oostenbrink, C.; Koller, J.; van Gunsteren, W. F. *Nucleic Acids Res.* **2005**, *33*, 725−733.
(33) Schneider, B.; Patel, K.; Berman, H. M. *Biophys. J.* **1998**, *75*, 2422−2434.
(34) Fujita, K.; MacFarlane, D. R.; Forsyth, M. *Chem. Commun.* **2005**, 4804−4806.
(35) Fujita, K.; MacFarlane, D. R.; Forsyth, M.; Fujita, M. Y.; Murata, K.; Nakamura, N.; Ohno, H. *Biomacromolecules* **2007**, *8*, 2080−2086.
(36) Drew, H. R.; Dickerson, R. E. *J. Mol. Biol.* **1981**, *151*, 535−556.
(37) Arai, S.; Chatake, T.; Ohhara, T.; Kurihara, K.; Tanaka, I.; Suzuki, N.; Fujimoto, Z.; Mizuno, H.; Niimura, N. *Nucleic Acids Res.* **2005**, *33*, 3017−3024.
(38) Subramanian, P. S.; Ravishanker, G.; Beveridge, D. L. *Proc. Natl. Acad. Sci. U.S.A.* **1988**, *85*, 1836−1840.
(39) Chalikian, T. V.; Eric Plum, G.; Sarvazyan, A. P.; Breslauer, K. J. *Biochemistry* **1994**, *33*, 8629−8640.
(40) Jordan, C. F.; Lerman, L. S.; Venable, J. H., Jr. *Nat. New Biol.* **1972**, *236*, 67−70.
(41) Parodi, S.; Kendall, F.; Nicolini, C. *Nucleic Acids Res.* **1975**, *2*, 477−486.
(42) Sinha, R.; Islam, M. M.; Bhadra, K.; Kumar, G. S.; Banerjee, A.; Maiti, M. *Bioorg. Med. Chem.* **2006**, *14*, 800−814.
(43) Lavelle, N.; Lee, S. A.; Flox, L. S. *Phys. Rev.* **1991**, *43*, 3126−3130.